A statistical study of the geoeffectiveness of magnetic clouds during high solar activity years

Jichun Zhang, Michael W. Liemohn, Janet U. Kozyra, Benjamin J. Lynch, and Thomas H. Zurbuchen

Space Physics Research Laboratory, University of Michigan, Ann Arbor, Michigan, USA

Received 29 January 2004; revised 14 May 2004; accepted 14 July 2004; published 15 September 2004.

[1] Using the *Dst* value corrected for the effects of magnetopause currents (*Dst**) and solar wind magnetic field and plasma data from 1 January 1998 to 30 April 2002, during elevated solar conditions, we have statistically examined the relationship of 271 storms ($Dst^* \leq -30$ nT) to 104 magnetic clouds. It is found that most of the magnetic clouds result in geomagnetic storms, but only about 30% of storms are due to magnetic clouds. A storm can be driven by a cloud's various regions or their combinations with dissimilar occurrence percentages. These percentages change as a function of geomagnetic activity levels as well. It is found that the leading field is the most geoeffective region and the sheath region is equally effective at causing magnetic storms during solar maximum (42%) compared to solar minimum (43%) as a percentage of magnetic cloud-induced storms. The occurrence percentage of intense storms caused by clouds is 72%, which is much higher than the ~20% occurrence percentage of smaller storms caused by clouds. It is also found that "unipolar B_z" and "bipolar B_z" clouds have different geoeffectiveness percentages, depending on the B_z orientation. The long-known control of magnetic activity mainly by southward B_z is supported by the results of this study. It is also shown that multistep development storms can result not only from both the combinations of sheath and cloud fields but also from different fields within a cloud. A new name, quasi-cloud, is proposed for those cloud-like solar wind structures which show evidence of relatively organized field rotations. *INDEX TERMS:* 7513 Solar Physics, Astrophysics, and Astronomy: Coronal mass ejections; 7524 Solar Physics, Astrophysics, and Astronomy: Magnetic fields; 7536 Solar Physics, Astrophysics, and Astronomy: Solar activity cycle (2162); 2788 Magnetospheric Physics: Storms and substorms; 2784 Magnetospheric Physics: Solar wind/magnetosphere interactions; *KEYWORDS:* magnetic cloud, *Dst* index, storms, solar wind–magnetospheric interactions, space weather

Citation: Zhang, J.-Ch., M. W. Liemohn, J. U. Kozyra, B. J. Lynch, and T. H. Zurbuchen (2004), A statistical study of the geoeffectiveness of magnetic clouds during high solar activity years, *J. Geophys. Res.*, *109*, A09101, doi:10.1029/2004JA010410.

1. Introduction

[2] A magnetic cloud is a transient ejection in the solar wind defined by relatively strong interplanetary magnetic fields (IMF), a large and smooth rotation of the magnetic field direction over approximately 0.25 AU at 1 AU, and an unusually low proton temperature [*Burlaga et al.*, 1981]. The duration of a typical magnetic cloud event at 1 AU can vary from several hours to days [*Lepping and Berdichevsky*, 2000; *Lynch et al.*, 2003]. A cloud is usually expanding as it moves outward from the Sun, as seen at 1 AU in its speed profile, i.e., from high to low speed [*Burlaga et al.*, 1981; *Farrugia et al.*, 1992; *Lepping et al.*, 2001].

[3] The orientation of magnetic cloud field configuration is determined by the coronal magnetic field. In order to quantify that relation, *Bothmer and Schwenn* [1998] interpreted the structures of magnetic clouds lying in the ecliptic plane as belonging to one of four categories (SWN, NES, SEN, and NWS) corresponding to the leading and trailing north-south magnetic field polarities and the east-west magnetic field in the center of the rope axial east-west magnetic field, where N, S, E, W is "North," "South," "East," and "West," respectively. *Mulligan and Russell* [1998] added four more categories (WNE, ESW, ENW, and WSE) with their axes perpendicular to the ecliptic plane. All eight categories are approximations of the cylindrical geometry and orientation derived from simple modeling of the internal field rotation and cloud orientation [e.g., *Lepping et al.*, 1990; *Lynch et al.*, 2003].

[4] SWN, NES, SEN, or NWS clouds are also called "bipolar B_z" clouds and WNE, ESW, ENW, or WSE are called "unipolar B_z" clouds. "Unipolar B_z" clouds include N and S magnetic clouds, where N means northward and S southward in the axial fields of the clouds. "Bipolar B_z" clouds include SN and NS magnetic clouds, where SN means from southward (in the leading fields) to northward (in the trailing fields) rotation in the magnetic field of the cloud events and NS from northward (in the leading fields) to southward (in the trailing fields) rotation in the magnetic

0148-0227/04/2004JA010410$09.00

field of the clouds [*Mulligan and Russell*, 1998]. There is a correlation between the preference of magnetic field rotations in magnetic clouds and the phase of a solar cycle [*Zhang and Burlaga*, 1988; *Bothmer and Schwenn*, 1998; *Mulligan and Russell*, 1998; *Zhao and Webb*, 2003; *Li and Luhmann*, 2004].

[5] It has been empirically shown [*Gonzalez and Tsurutani*, 1987] that intense storms with peak $Dst \leq -100$ nT are primarily caused by large $B_z \leq -10$ nT fields with duration greater than 3 hours. The thresholds of B_z and duration for moderate and small storms at the 80% occurrence level are -5 nT, 2 hours and -3 nT, 1 hour, respectively [*Russell et al.*, 1974; *Gonzalez et al.*, 1994]. Interplanetary electric field E_y is also one of the popular solar wind-magnetosphere coupling functions. Magnetic clouds are ideal objects for solar-terrestrial studies because of their simplicity and their extended intervals of southward and northward magnetic fields [*Burlaga et al.*, 1990; *Zhao and Hoeksema*, 1998; *Huttunen et al.*, 2002]. The geomagnetic response to magnetic clouds is reviewed by *Farrugia et al.* [1997, 1998].

[6] Geomagnetic storms, especially intense ones, can severely affect space-borne [*Lundstedt et al.*, 1995] and ground-based technological systems [*Lundstedt*, 1992; *Boteler*, 1993; *Viljanen and Pirjola*, 1994]. Magnetic clouds and the possible sheath fields ahead of them are one of major origins of southward-directed interplanetary magnetic fields [*Gonzalez et al.*, 1994]. It is therefore of significant economic and social importance, and also a great scientific challenge, to study the geoeffectiveness of near-Earth magnetic clouds.

[7] After investigating thirty-four magnetic clouds observed by Wind when it is not in the magnetosphere of the Earth during low solar activity years (1995–1998), *Wu and Lepping* [2002] found that a geomagnetic storm can be induced by a sheath, the leading field, or the trailing field of a cloud. They found that a cloud's leading field was a major driving force for storms in that phase of the solar cycle by comparing the geoeffectiveness of the sheaths and different fields of those clouds. As in the previous studies [*Tsurutani and Gonzalez*, 1997; *Huttunen et al.*, 2002; *Vieira et al.*, 2001; *Gonzalez et al.*, 2001], they also showed that a multistep main phase storm [*Kamide et al.*, 1998] could be caused by the combination of a sheath and cloud structure. But, in the study of *Wu and Lepping* [2002], only "bipolar B_z" (SN or NS) magnetic clouds are investigated and a cloud is divided into only two regions, the leading and trailing field, and the axial field is omitted as a separate category.

[8] Magnetic clouds are a specialized subset of interplanetary coronal mass ejections (ICMEs) comprising anywhere from one-third [*Gosling*, 1990] to one-half [*Cane et al.*, 1997] of all ICME events. The internal helical field structure of magnetic clouds has an extensive history of being modeled by relatively simple force-free magnetic field solutions [*Goldstein*, 1983; *Marubashi*, 1986; *Burlaga*, 1988; *Lepping et al.*, 1990]. However, *Cane and Richardson* [2003] present many ICME events with evidence of somewhat organized field structure, but have not been reported as magnetic clouds. Because most of these events are found to be geoeffective ($Dst^* \leq -30$ nT), they are included in our study. We propose a new name for these and other cloud-like (R. P. Lepping, private communication, 2003) structures, quasi-clouds.

[9] *Wu and Lepping* [2002] found that 38% of solar minimum magnetic clouds produced storms driven by the sheath passage (either partially or fully). During solar minimum, the heliospheric current sheet is relatively smooth and well behaved, with the classic "ballerina skirt" appearance. During solar maximum, however, the current sheet becomes highly distorted from the classic picture, with a severely warped topology and a highly inclined tilt [*Zhao and Webb*, 2003]. Thus the ambient solar wind being compressed in the sheath is quite different at solar minimum and maximum. A hypothesis (to be tested in the present study) is that the sheath region will cause more storms during solar maximum than solar minimum.

[10] In this study, almost continuous solar wind IMF and plasma data from the Advanced Composition Explorer (ACE) are used to identify all magnetic cloud events in high solar activity years from 1 January 1998 to 30 April 2002. This time period is chosen as the solar maximum complement to the solar minimum interval examined by *Wu and Lepping* [2002]. By only considering the B_z rotation, we classify these magnetic cloud events into four categories: S, N, SN and NS magnetic clouds. All geomagnetic storms ($Dst^* \leq -30$ nT) during this period are also identified and subdivided into three levels of geomagnetic activity (weak storms (-50 nT $< Dst^* \leq -30$ nT), moderate storms (-100 nT $< Dst^* \leq -50$ nT) and intense storms ($Dst^* \leq -100$ nT)). Finally, the relationships between the magnetic clouds and geomagnetic storms are statistically studied.

2. Data Processing

[11] Four-minute IMF data (MAG, level 2) and 64-s solar wind plasma parameters (SWEPAM, level 2) were obtained from the ACE Science Center. The plasma data were then averaged to 4-min resolution, taking any 64-s value whose start minute fell between the start minute of the IMF data and 4 minutes later. All the solar wind IMF and plasma data were transferred from GSE to GSM coordinates with GEOPACK (N. A. Tsyganenko, A set of FORTRAN subroutines for computations of the geomagnetic field in the Earth's magnetosphere, http://www-istp.gsfc.nasa.gov/Modeling/geopack.html, 2001).

[12] Hourly *Dst* indices were downloaded from the World Data Center, Kyoto and then corrected to remove the effects of the solar wind dynamic pressure [*Gonzalez et al.*, 1994]:

$$Dst^* = Dst - b\left(nV^2\right)^{1/2} + c$$

where $b = 0.02$ nT/(cm^{-3} km^2/s^2)$^{1/2}$ and $c = 20$ nT. n and V are one-hour resolution solar wind number density and bulk flow speed, respectively.

[13] The pressure corrected *Dst* index (Dst^*) is obtained by removing the contributions to the disturbance field at the Earth's surface from the magnetopause currents, and thus contains mainly the inner magnetospheric contribution due to the ring current build-up and decay.

[14] Before the *Dst* pressure-corrected calculation, the solar wind density n and bulk flow speed V data were shifted from the ACE spacecraft position, the Sun-Earth

Table 1. Near-Earth Magnetic Cloud List, 1 January 1998 to 30 April 2002

	Start Time		End Time			*Dst**,		
Year	(DOY)	Hour	(DOY)	Hour	Quality[a]	nT	Class.	Polarity
98	(007)[b]	0.8	(008)	10.0	2	−85	S & LF[c]	SN[d]
98	(008)	14.0	(008)	22.1	3	#	#	SN
98	020	17.2	021	3.9	2	−41	S & LF	SN
98[e]	021	5.5	022	11.1	2	#	#	N
98	(035)	4.8	(036)	22.0	3	#	#	SN
98	048	10.0	049	14.7	2	−117	AF	S
98	049	22.8	051	0.0	2	−50	TF	NS
98	(063)	13.1	(065)	6.2	1	−46	LF	N
98	065	22.9	066	11.5	2	#	#	SN
98[e]	084	16.2	085	9.0	2	−63	Sheath	N
98	(122)	11.9	(123)	16.9	2	−101	S & LF	SN
98	(153)	10.5	(153)	15.9	1	#	#	N
98	165	3.9	166	7.1	3	−56	LF	SN
98	(175)	16.8	(176)	21.8	2	−48	LF	SN
98	212	4.9	212	16.2	3	−48	S & LF	SN
98	213	12.9	215	3.0	3	#	#	N
98	217	13.2	218	12.0	2	−164	TF	NS
98[e]	220	1.8	222	0.1	2	#	#	SN
98	224	1.2	225	13.3	3	#	#	NS
98	(232)	7.9	(233)	18.6	1	−70	S & LF	SN
98[e]	239	5.4	240	0.3	2	−170	AF	S
98	(268)	5.9	(269)	16.0	3	−229	S & LF	SN
98	(292)	4.0	(293)	7.1	2	−113	S & LF	SN
98	311	22.0	312	12.5	2	−163	LF	SN
98	(312)	18.8	(314)	1.7	2	−150	TF & TF	NS
99	013	15.8	013	22.3	1	−134	AF	S
99	(049)	14.2	(050)	11.2	1	−138	Sheath	SN
99[e]	059	14.0	060	15.9	2	−113	LF	SN
99	(106)	18.1	(107)	21.0	2	−106	LF	SN
99	111	4.3	112	15.2	2	−32	LF	SN
99	153	22.6	154	22.0	2	#	#	N
99	177	2.3	177	19.5	2	#	#	SN
99	189	1.8	190	4.2	3	−31	TF	NS
99	208	20.0	210	4.8	2	−38	TF	NS
99	212	18.7	214	4.0	2	−47	LF	SN
99	(220)	17.6	(222)	18.0	1	−50	S & LF	SN
99	233	5.6	235	16.0	2	−70	TF	NS
99	(264)	18.2	(265)	11.7	2	−35	LF	SN
99[e]	316	9.4	317	22.2	3	−106	TF & TF	NS
99	346	20.0	347	16.0	3	−87	AF	S
99	361	11.3	362	4.7	2	#	#	NS
00	022	17.1	023	1.8	2	−120	AF	S
00	(043)	12.0	(044)	0.6	3	−158	Sheath	SN
00	(052)	4.3	(053)	13.3	1	#	#	N
00	070	0.9	070	5.5	2	#	#	N
00	098	6.8	099	18.0	2	−337	Sheath	NS
00	118	18.0	119	1.0	3	−38	TF	NS
00	137	23.2	138	7.5	3	−112	LF	SN
00	145	12.1	148	10.4	3	−178	Sheath	S
00	157	0.0	158	22.7	3	−51	S & LF	SN
00	163	7.2	163	17.8	2	−45	LF & LF	SN
00	170	4.0	170	16.7	3	#	#	NS
00	183	7.5	185	7.0	3	#	#	NS
00	193	23.2	195	9.1	2	−38	S & LF	SN
00	(196)	17.0	(197)	14.1	2	−81	S & TF	NS
00	(197)	19.4	(198)	10.0	1	−339	LF	SN
00	209	2.1	210	5.4	1	−67	S & TF	NS
00	(210)	12.1	(211)	12.0	2	−83	LF & TF	N
00	(213)	22.0	(214)	15.8	2	−48	S & TF	NS
00	223	19.3	224	18.0	1	−98	AF	S
00	(225)	5.5	(226)	22.2	1	−244	S & LF	SN
00[e]	246	21.9	247	12.7	3	−57	Sheath	N
00	(261)	23.4	(265)	0.0	3	−235	Sheath	NS
00	(277)	10.2	(279)	2.5	1	−218	S & TF	NS
00	(287)	6.1	(288)	16.5	1	−107	S & TF	NS
00	(302)	20.5	(304)	22.3	3	−127	LF	SN
00	(311)	22.0	(312)	18.0	2	−187	S & LF	SN
00	333	16.0	334	20.2	2	−128	AF	S
00	357	19.7	359	17.0	3	−62[f]	LF	SN
01	024	8.8	025	14.0	3	−56	LF	SN
01[e]	063	15.7	064	1.6	3	−78	TF	NS
01	(078)	17.0	(081)	9.5	1	−163	S & LF	SN
01	090	5.0	090	22.5	3	−394	LF	SN
01	(094)	21.3	(095)	8.3	3	−39	TF	NS
01	(101)	21.3	(102)	7.0	3	−296	LF	SN
01[e]	103	10.2	104	11.6	2	−81	Sheath	SN
01	(111)	23.6	(113)	8.3	1	−108	AF	S
01	127	17.9	128	7.9	3	#	#	NS
01	129	11.9	130	21.6	2	−73	S & LF	SN
01	136	7.1	136	23.8	3	#	#	NS
01	(148)	3.9	(149)	21.1	1	−40	LF	SN
01	150	7.9	151	9.2	3	#	#	SN
01	158	18.0	159	6.5	3	#	#	N
01	172	3.1	172	10.2	3	#	#	S
01	(190)	2.1	(192)	3.9	1	−36	S & TF	NS
01	194	17.0	195	1.1	2	−31	AF	S
01	242	11.6	243	10.0	3	−45	TF	NS
01	244	16.1	245	22.5	2	#	#	NS
01	256	17.7	257	22.8	3	#	#	N
01	266	23.9	268	0.0	3	#	#	N
01	273	0.9	273	18.8	2	−93	TF	N
01	275	23.5	276	16.3	1	−182	TF	NS
01	285	2.2	285	10.9	2	−96	LF	SN
01	(304)	18.0	(306)	11.1	2	−92	S & LF	SN
01	323	22.9	324	11.0	3	−44	LF	SN
01	(328)	13.8	(329)	11.3	2	−252	Sheath	N
01	364	0.1	364	14.6	3	−47	LF	SN
02	046	11.0	047	3.0	3	#	#	NS
02	047	7.8	047	21.9	3	#	#	SN
02	059	16.7	060	9.6	1	−73	LF	SN
02	(078)	4.5	(079)	12.6	1	−42	LF	SN
02	(083)	10.8	(084)	20.8	1	−112	S & LF	SN
02	107	21.5	109	8.0	1	−142	S & LF	SN
02	(110)	4.4	(111)	17.5	3	−171	Sheath	SN

[a]Quality, measured subjectively with respect to the definition of *Burlaga* [1991]: 1, excellent, 2, good, 3, poor.

[b]A magnetic cloud, whose DOY is in parentheses, has been reported as an event which can be modeled by a force-free flux rope.

[c]S is the sheath; LF is the leading field; AF is the axial field; TF is the trailing field.

[d]N is north; S is south.

[e]A magnetic cloud that is not listed by *Cane and Richardson* [2003].

[f]Since n is missing, *Dst** cannot be computed and is substituted by the value of *Dst*.

Lagrange-1 (or L1) point, to the magnetopause of the Earth with fixed time, one hour. To fill in solar wind data gaps, ACE observations were supplemented by Wind and IMP-8 observations from the OMNI data set. However, there is still one magnetic cloud event in which the solar wind density is missing. For this event (noted in Table 1), it was not possible to calculate *Dst** so *Dst* was used instead.

[15] The storm strength was gauged by the *Dst* index because the use of *Dst* is well known to help identify and quantify magnetic storms [*Gonzalez et al.*, 1994; *Huttunen et al.*, 2002]. Moreover, geomagnetic storms can be categorized by their intensity. We have applied the *Gonzalez et al.* [1994] intensity categories to the *Dst** index. During the period of 1 January 1998 to 30 April 2002, 50 intense storms ($Dst^* \leq -100$ nT), 108 moderate storms (-100 nT $< Dst^* \leq -50$ nT) and 113 weak storms (-50 nT $< Dst^* \leq -30$ nT) were identified.

[16] The identification criteria for a magnetic cloud are: (1) the magnetic field direction undergoes a smooth, monotonic rotation over a large angle, (2) the magnetic field

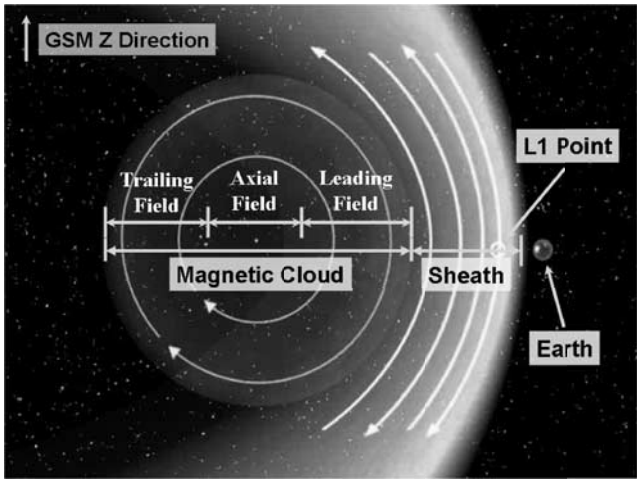

Figure 1. Schematic diagram of the geometry of a "bipolar B_z" SN magnetic cloud and the magnetic field lines in the sheath and magnetic cloud in the XZ plane of GSM coordinates whose positive Z direction is denoted by "North." The magnetic cloud is divided into three regions in no scale: the leading, axial, and trailing field; the position of the ACE spacecraft and Earth is also indicated.

strength is higher than average, and (3) the temperature is lower than average [*Burlaga*, 1991]. Using the above three cloud features, and guidelines in choosing the boundaries of a cloud event [*Lepping et al.*, 1990; *Wei et al.*, 2003], 104 clouds were identified in the ACE data from 1 January 1998 to 30 April 2002. A sheath can be identified ahead of most of these magnetic cloud events. The signatures of the sheath region are enhanced magnetic field strength and rapidly varying field direction, as well as increased particle temperature, density, and speed [*Tsurutani et al.*, 1988]. The leading "boundary" of the sheath can be a shock, a shock-like structure, pressure pulse, or a sharp rise in density, temperature or velocity [*Wu and Lepping*, 2002]. In our study, all cloud events are divided into three regions: leading field, axial field and trailing field. Moreover, on the basis of the magnetic field rotations in the different regions of the clouds, magnetic cloud events are called "unipolar B_z" (N and S) or "bipolar B_z" (SN and NS) magnetic clouds [*Mulligan and Russell*, 1998]. Figure 1 is a schematic drawing of a magnetic cloud approaching the Earth. It shows the geometry of a "bipolar B_z" SN cloud, which acts like a magnetic flux rope [*Gosling*, 1990] and has an upstream sheath and a smoothly south-to-north (SN) rotation in B_z, in the XZ plane of GSM coordinates whose positive Z direction is denoted. The three regions in the cloud, the leading field, axial field and trailing field, are indicated but not in scale; the position of the L1 point and Earth is also indicated. Figure 1 also shows strong field oscillation and hotter and denser plasma in the sheath region than in the cloud itself.

[17] All of the 104 magnetic cloud events studied are listed in Table 1. We refer to a number of existing magnetic cloud and ICME lists, including Wind magnetic clouds (http://lepmfi.gsfc.nasa.gov/mfi/mag_cloud_pub1.html), ACE magnetic clouds [*Lynch et al.*, 2003; B. J. Lynch, private communication, 2003], and a subset of the more general list of ICMEs [*Cane and Richardson*, 2003] that exhibit some sort of organized field structure. A vast majority of the *Lynch et al.* [2003] events are included with some modification of the boundaries because we are no longer constrained by selecting the most conservative interval that is well-approximated by the cylindrical, linear force-free magnetic field model. In fact, many events listed here cannot be fit with a simple field model. The remaining differences between the two lists are due to the data resolution, i.e., smooth rotations or low proton temperature in 1-hour data were sometimes less smooth or low in 4-min data, and events $\leq$10 hours were not resolved by *Lynch et al.* [2003]. Nine additional cloud-like events were identified and added to the list, because these events, along with the cloud-like event subset of the *Cane and Richardson* [2003] list ("MC 1"), have relatively smooth and extended intervals of southward and northward magnetic fields and are thus ideal objects for solar-terrestrial studies.

[18] The first five columns in Table 1 give the year, estimated start and end times of the magnetic cloud events, respectively, while the following column indicates the quality of the events (1, excellent; 2, good; 3, poor). The quality of the events is determined by how they conform to the above identification criteria of a magnetic cloud [*Burlaga*, 1991]. The sixth column gives the minimum value of the geomagnetic *Dst** index (stronger activity is denoted by an increasingly negative value), while a "#" denotes the event is not geoeffective and no storm is associated with it. The geoeffective regions of each cloud event are given in the second to last column. S is the sheath; LF is the leading field; AF is the axial field; TF is the trailing field. In the final column of Table 1, we indicate the B_z polarity of each event [*Mulligan and Russell*, 1998].

3. Cloud Region Drivers

[19] We find that a geomagnetic storm can be driven by the sheath, the leading field of a cloud, the trailing field of a cloud, or both sheath and cloud fields, which is consistent with the results of *Wu and Lepping* [2002]. However, we also find that the axial fields of some clouds are geoeffective (predicted by *Zhao and Hoeksema* [1998]) and that the leading or trailing field alone can cause a multistep storm.

[20] Figures 2a–2i shows solar wind and *Dst* or *Dst** variation during nine different magnetic cloud events. Table 2 summarizes the identified driving region, the associated storm complexity, and the magnetic cloud polarity type for each event. Figures 2a–2d show single-step storms, and Figures 2e–2i show multistep storms. The date and time of the minimum of the *Dst** index are denoted by the vertical dotted line in all panels and also shown in hour, DOY, and year order at the top of each figure. The boundaries of each magnetic cloud event are indicated with vertical solid lines and for events with identifiable sheath regions; another vertical solid line represents the location of the upstream shock.

[21] The panels in Figures 2a–2i from top to bottom are the interplanetary magnetic field magnitude ($|B|$), proton temperature (T), latitude and longitude of the solar wind magnetic field in RTN coordinates, north-south component of the IMF (B_z) in GSM coordinates, negative y component (in the west-east direction) of interplanetary electric field in

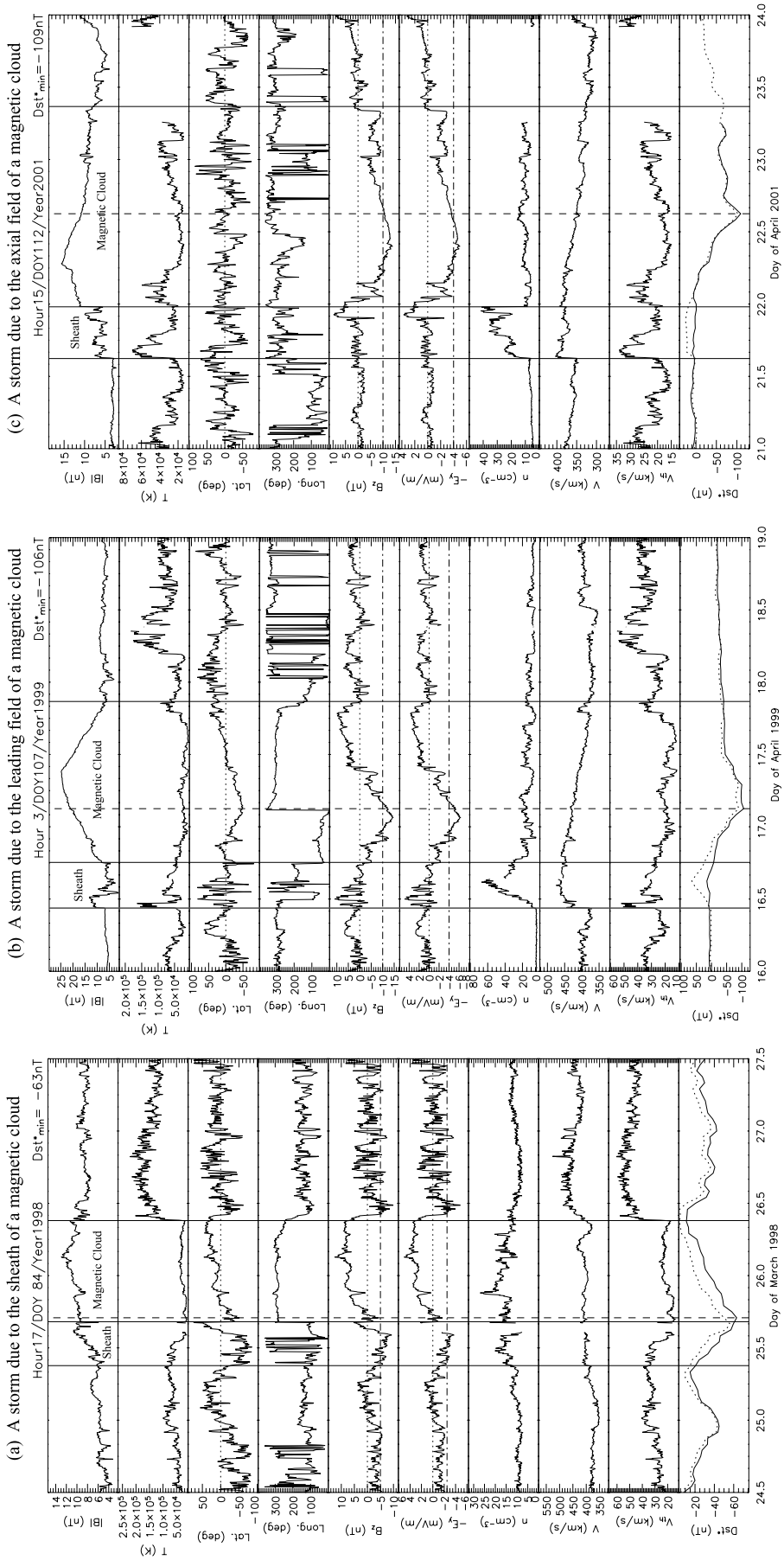
(a) A storm due to the sheath of a magnetic cloud
Hour17/DOY 84/Year1998
Dst*min = −63nT
(b) A storm due to the leading field of a magnetic cloud
Hour 3/DOY107/Year1999
Dst*min = −106nT
(c) A storm due to the axial field of a magnetic cloud
Hour15/DOY112/Year2001
Dst*min = −109nT
Sheath
Magnetic Cloud
T (K)
|B| (nT)
Lat. (deg)
Long. (deg)
Bz (nT)
−Ey (mV/m)
n (cm−3)
V (km/s)
Vsw (km/s)
Dst* (nT)
Day of March 1998
Day of April 1999
Day of April 2001

Figure 2

GSM coordinates ($-E_y$; where interplanetary electric field E_y is defined as $-VB_z \times 10^{-3}$ (mV/m)), proton density (n), plasma bulk speed (V), proton thermal speed (V_{th}), and geomagnetic indices *Dst* denoted by the dotted line and *Dst** by the solid line. The horizontal dot-dashed lines in B_z and $-E_y$ panels denote the thresholds for storms at the 80% occurrence level [*Gonzalez et al.*, 1994]. RTN is a spacecraft centered coordinate system (R is the Sun to the ACE spacecraft unit vector; T equals to $\Omega \times R/|\Omega \times R|$, where Ω is the Sun's spin axis in J2000 GCI; N completes the right-handed triad). J2000 GCI is the geocentric inertial reference frame using the Julian Epoch of Jan. 1, 2000. At the Julian Epoch, X is the Earth's mean vernal equinox and Z is the Earth's mean spin axis.

[22] The single-step storms (Figures 2a–2d) appear to have a relatively simple driving-response connection; the southward field found in different regions of the magnetic cloud or the sheath drives the magnetospheric response. The multistep storms are more complicated. Figures 2e and 2f show events that have southward field in both the sheath and cloud regions. Figure 2g shows the single event with leading and trailing southward fields, and Figures 2h and 2i have multistep storms probably driven by fluctuations in their southward field regions.

4. Statistical Results

[23] On the basis of the 104 cloud events investigated in this study, we found that the resulting geomagnetic storms were induced by the southward magnetic field sources from three more cloud configurations than the four cloud types of *Wu and Lepping* [2002]: (1) the sheath, (2) the cloud's leading field (LF), (3) the cloud's axial field (AF), (4) the trailing field of a cloud (TF), (5) both LF and TF, (6) both sheath and LF and (7) both sheath and TF. Figure 3 shows the percentages and subtotal of the cloud events for each of these seven categories. A two-step main phase storm can be induced by a combination of sheath and cloud fields, but the leading or trailing fields alone can also cause a multistep storm, although much less frequently.

[24] Figure 4 shows the intensity of the geomagnetic response to magnetic cloud and quasi-cloud input. These events result in weak, moderate, and intense storms, 20[4.4]%, 22[4.6]%, and 34[5.7]% of the time respectively, whereas 24[4.8]% of cloud and quasi-cloud events are not associated with geomagnetic storms. The numbers in parentheses are the $\sqrt{N}$ counting errors for each percentage. The $\sqrt{N}$ counting errors indicate that the no storm, weak storm, and moderate storm percentages are statistically identical, but the higher percentage for intense storms is statistically significant.

[25] However, Figure 5a shows that during our study, more than 70% (192 storms) of the total 271 storms ($Dst^* \leq -30$ nT) are not due to magnetic cloud events, which is consistent with the finding of *Li and Luhmann* [2004]. The percentages of the total storms which are caused by the various cloud region(s) are as follows: the sheath (3.7%, 10 storms), the leading field (8.5%, 23 storms), the axial field (3.3%, 9 storms), the trailing field (4.8%, 13 storms), both leading and trailing fields (0.4%, 1 storm), both sheath and leading field (6.3%, 17 storms), and both sheath and trailing fields (2.2%, 6 storms).

[26] Figures 5b, 5c, and 5d show the occurrence percentages of three levels of geomagnetic activity induced by ithe different regions of magnetic clouds. It is very apparent that the different levels of geomagnetic activity caused by magnetic clouds have dissimilar occurrence percentages due to different cloud regions. For weak storms, activity is dominated by the leading fields of clouds; for moderate storms, activity is dominated by either leading fields or sheath/cloud leading field combinations and sheaths and axial fields become important; as for intense storms, sheaths and axial fields become even more important and have almost the same occurrence percentages as leading fields or sheath/cloud leading field combinations. It is also illustrated in Figure 5 that the roles played by trailing fields or sheath/cloud trailing field combinations do not change much with storm intensity.

[27] The occurrence percentage 70[11.8]% of intense storms caused by magnetic clouds is extraordinary high, compared with lower geomagnetic activities (weak: 19[4.1]%; moderate: 21[4.4]%). In other words, magnetic clouds dominate intense storm occurrences.

[28] In order to study the geoeffectiveness of "bipolar B_z" and "unipolar B_z" clouds, we divided the 104 cloud events into four classifications: SN, NS, S and N clouds [*Mulligan and Russell*, 1998]. In the period of from 1 January 1998 to 30 April 2002, almost 48%, 27%, 14% and 11% of the 104 cloud events are SN, NS, S and N clouds (50, 28, 15 and 11 events), respectively, which is consistent with the findings of *Mulligan and Russell* [1998].

[29] Figure 6 shows the occurrence percentages of different levels of geomagnetic activity induced by SN, NS, S and N magnetic clouds. More than 90[28.7]% of S clouds, but only about 40[16.3]% of N clouds, cause geomagnetic storms. This is a statistically significant difference. The percentage of SN clouds that do not cause storms is only half of that in NS clouds. About 25% of "bipolar B_z" clouds and 10% of "unipolar B_z" clouds result in weak storms. S and NS clouds have the same occurrence percentages of moderate storms, which is a little lower than that in SN and N clouds. More than 60% of S clouds cause intense storms through their prolonged axial southward magnetic fields,

Figure 2. (a–c) Observations by the ACE spacecraft and *Dst** for the nine magnetic cloud events: (a) 25 March 1998, (b) 16 April 1999, and (c) 21 April 2001. From top to bottom are plotted interplanetary magnetic field magnitude (|B|), proton temperature (T), latitude in RTN coordinates, longitude in RTN coordinates, north-south component of the IMF (B_z), negative y component of interplanetary electric field ($-E_y$), proton density (n), plasma bulk speed (V), proton thermal speed (V_{th}), and geomagnetic indices *Dst* denoted by the dotted line and *Dst** denoted by the solid line. The horizontal dot-dashed lines in B_z and $-E_y$ panels denote the thresholds for storms at the 80% occurrence level [*Gonzalez et al.*, 1994]. (d–f) Same as Figures 2a–2c but for the magnetic cloud events: (d) 2 October 2001, (e) 12 August 2000, and (f) 31 July 2000. (g–i) Same as Figures 2a–2c but for the magnetic cloud events: (g) 28 July 2000, (h) 11 June 2000, and (i) 8 November 1998.

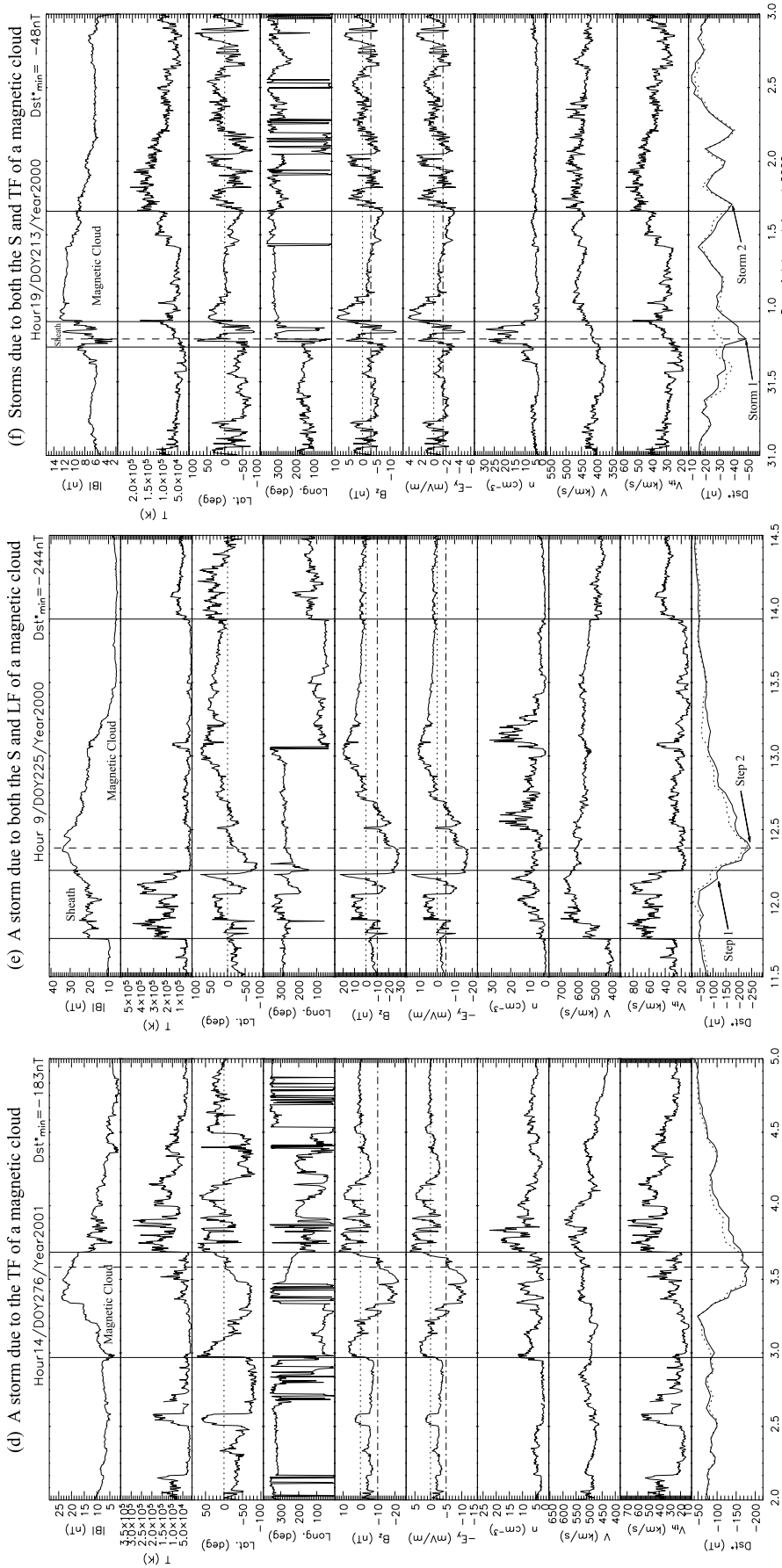

Figure 2. (continued)

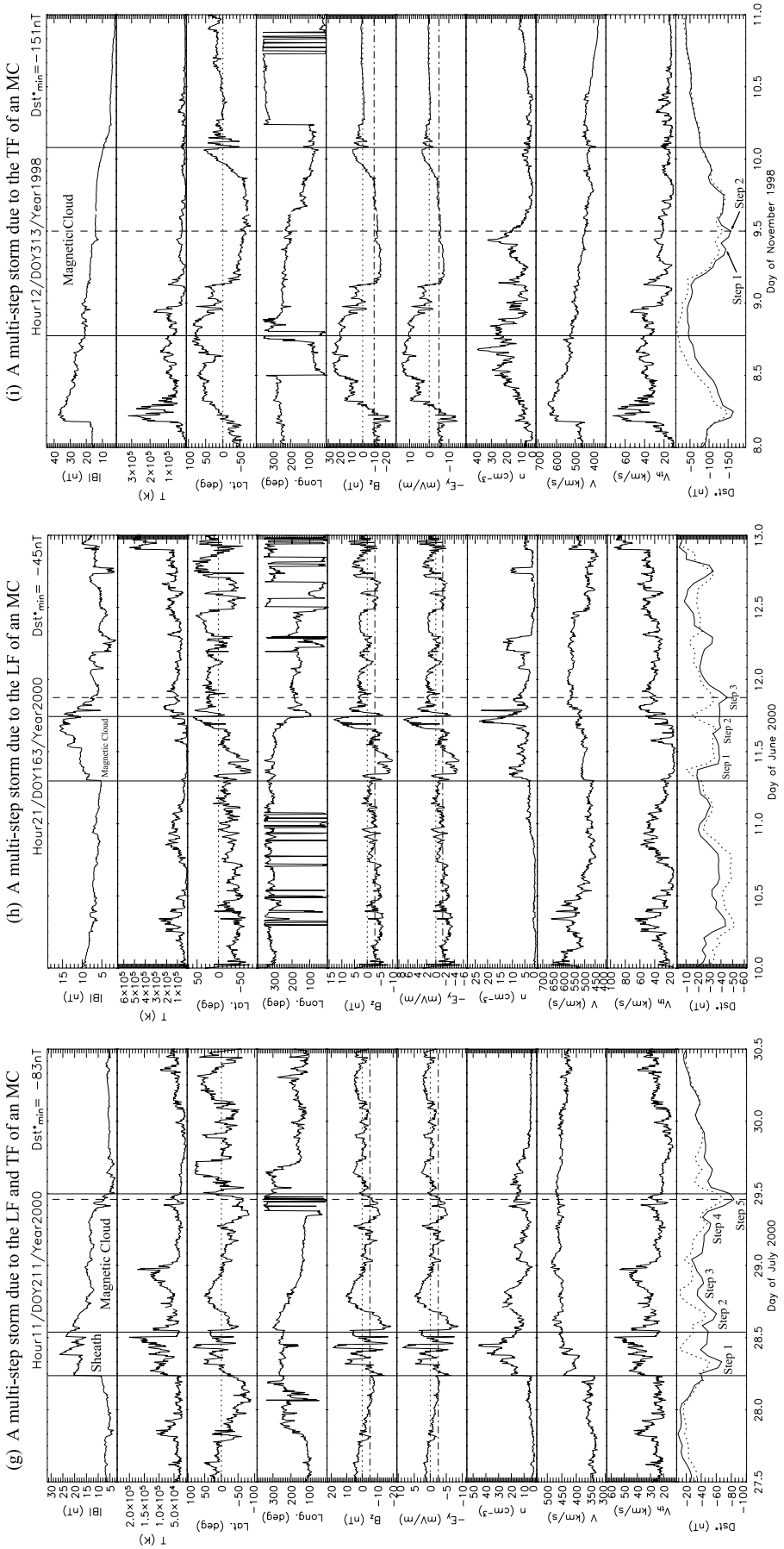

Figure 2. (continued)

Table 2. Figures 2a–2i Summary

Figure	Date	Driver Class.	Complexity	B_z Polarity
2a	25 March 98	Sheath (S)	single-step	unipolar N
2b	16 April 99	Leading Field (LF)	single-step	bipolar SN
2c	21 April 01	Axial Field (AF)	single-step	unipolar S
2d	2 Oct. 01	Trailing Field (TF)	single-step	bipolar NS
2e	12 Aug. 00	S & LF	multistep	bipolar SN
2f	31 July 00	S & TF	multistep	bipolar NS
2g	28 July 00	LF & TF	multistep	unipolar N
2h	11 June 00	LF	multistep	bipolar SN
2i	8 Nov. 98	TF	multistep	bipolar NS

while less than 10% of N clouds are associated with intense storms. As for SN and NS clouds, the occurrence percentages of intense storms are about 40% and 30%, respectively. In general, the strength of the storms is not found to be significantly different between the SN and NS cloud, which is consistent with *Wilson* [1987].

[30] Figure 7 illustrates the occurrence percentages of all levels of geomagnetic activity caused by the different fields of "bipolar B_z" and "unipolar B_z" magnetic clouds. Sheaths are geoeffective in all types of clouds, but the occurrence percentages of storms due to sheaths are not high in S, SN, and NS clouds (about 10%), except in N clouds (about 20%). The axial, leading, and trailing fields are the most geoeffective regions in S, SN, and NS clouds, respectively. Both leading and trailing fields are geoeffective in N clouds, but the occurrence percentages of storms due to these regions are all low, about 7%. More than 80% of S clouds cause storms by just their axial fields, but only about half of SN clouds and 40% of NS clouds result in storms through their leading or trailing fields. For SN or NS clouds, more storms were caused by leading or trailing fields than those by the combinations of sheaths and leading or trailing fields and the occurrence percentages are about 30% and 20%, respectively.

5. Discussion and Summary

[31] Using the *Dst** index and solar wind IMF & plasma data from 1 January 1998 to 30 April 2002 in which solar activities are high, we have statistically examined the relationship of 271 storms ($Dst^* \leq -30$ nT) and 104 magnetic clouds. It is found that nearly 80% of magnetic clouds can result in geomagnetic storms. As the resulting geomagnetic activity increases, so do the occurrence percentages (weak storms: 20.2%; moderate storms: 22.1%; intense storms: 33.7%).

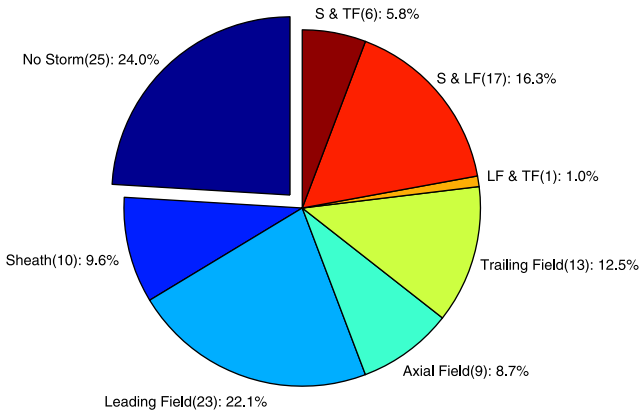

Figure 3. Pie plots showing the geoeffectiveness of the different fields of magnetic clouds: (1) the sheath, (2) the cloud's leading field (LF), (3) the cloud's axial field (AF), (4) the trailing field of a cloud (TF), (5) both LF and TF, (6) both sheath and LF, and (7) both sheath and TF. The number in parentheses is the subtotal of magnetic clouds in each category.

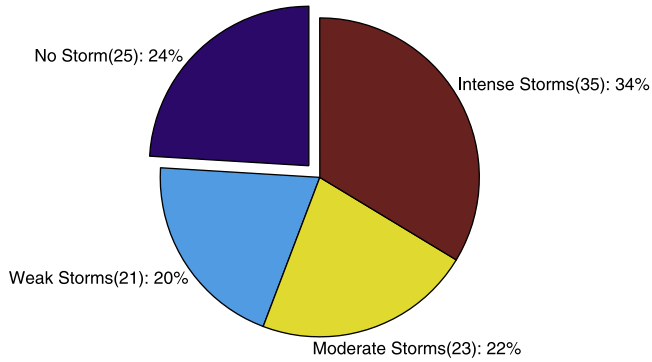

Figure 4. Pie plots showing the geoeffectiveness of magnetic clouds. The number in parentheses is the subtotal of magnetic clouds in each category.

5.1. Comparison With Solar Minimum

[32] A storm caused by a magnetic cloud can be induced by fields from any region of the cloud, the sheath, or some combination of thereof. This study is a good complement to *Wu and Lepping* [2002] in which magnetic cloud events from the first four years of Wind occur during low solar activity. We find that the cloud's leading field is a major driving force for storms during the high solar activity years, in agreement with the *Wu and Lepping* [2002] results for solar minimum.

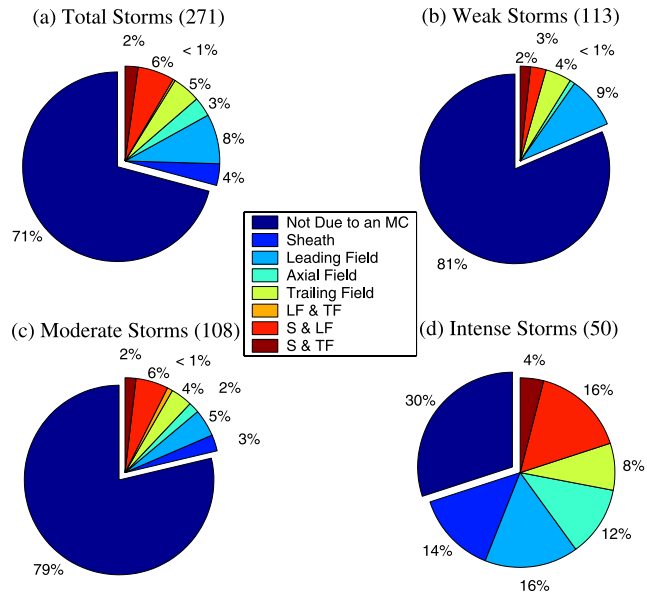

Figure 5. Pie plots showing the occurrence percentages of different levels of geomagnetic activity due to the different fields of magnetic clouds: (a) weak storms, (b) moderate storms, and (c) intense storms. The subtotal of each kind of storms is in parentheses in the respective title.

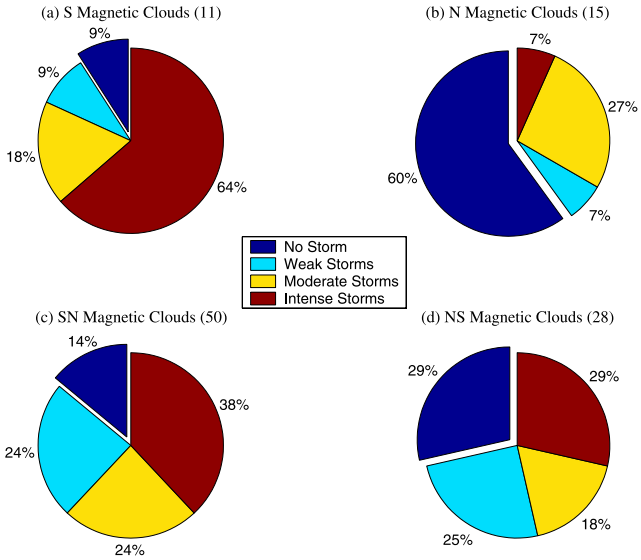

Figure 6. Pie plots showing the occurrence percentages of different levels of geomagnetic activity due to "bipolar B_z" and "unipolar B_z" magnetic clouds: (a) S magnetic clouds, (b) N magnetic clouds, (c) SN magnetic clouds, and (d) NS magnetic clouds. The subtotal of each type of magnetic clouds is in parentheses in the respective title.

[33] The hypothesis formulated in the Introduction was that the sheath region of magnetic clouds cause more storms during solar maximum than solar minimum. The present study found that 32[5.5]% of the MC sheaths during solar maximum caused storms (either partially or fully). The similar number from solar minimum was 38[10.6]%. However, when viewed as a percentage of MC-induced storms (a slightly smaller denominator), the sheath-induced storms are 42[7.3]% and 43[12.0]% for solar maximum and minimum, respectively. The null hypothesis is correct: sheath regions are equally geoeffective during solar maximum and solar minimum (as defined by the two studies).

5.2. Magnetic Storms and Magnetic Clouds

[34] More than 70% of storms are not due to magnetic clouds, even though we include both the traditional magnetic cloud events and those events which we have labeled quasi-clouds [e.g., *Cane and Richardson*, 2003]. Therefore it is not adequate to study only the geoeffectiveness of magnetic clouds and cloud-like ejecta in predicting storms in space weather applications. It is important to include other geoeffective sources in the solar wind, such as corotating interaction regions (CIRs) and those non cloud-like ICMEs, in the study of solar wind-terrestrial interactions.

[35] The different levels of geomagnetic activity caused by magnetic clouds have dissimilar occurrence percentages due to different cloud regions. For weak storms, activity is dominated by the leading fields of clouds; for moderate storms, by either leading fields or sheath/cloud leading field combinations and sheaths and axial fields become important; and for intense storms, sheaths and axial fields become even more important and have almost the same occurrence percentages as leading fields or sheath/cloud leading field combinations. It is also found that, as storms become more intense, the roles played by trailing fields or sheath/cloud trailing field combinations do not change much.

[36] The occurrence percentage (70%) of intense storms caused by magnetic clouds is extraordinary high, compared with lower geomagnetic activity (weak: 19%; moderate: 21%). In other words, magnetic clouds dominate intense storm occurrences.

5.3. Comparison of Magnetic Cloud Types

[37] By subdividing the total cloud events into S, N, SN and NS clouds, the correlation of magnetic clouds with different rotations in B_z to storms of various intensities is established. It is found that "unipolar B_z" and "bipolar B_z" clouds have different geoeffectiveness percentages. In general, the strength of the storms is not found to be significantly different for the SN and NS clouds, but intense storms dominate in S clouds and moderate storms in N clouds, which are in agreement with the results of *Vieira et al.* [2001]. It is apparent that southward B_z determines the geoeffective regions in a "unipolar B_z" or "bipolar B_z" magnetic cloud structure and the long-known hypothesis that geomagnetic activity is mainly controlled by southward B_z is supported by the results of this study.

[38] Different from the results in previous studies [*Tsurutani and Gonzalez*, 1997; *Gonzalez et al.*, 2001; *Wu and Lepping*, 2002] in which multistep main phase development storms can only be due to the combinations of sheath and cloud fields, it is shown in this study that multistep storms can also result from different component fields within the cloud itself.

[39] A new name, quasi-cloud, is proposed for those cloud-like solar wind structures (R. P., Lepping, private communication, 2003) which show evidence of relatively

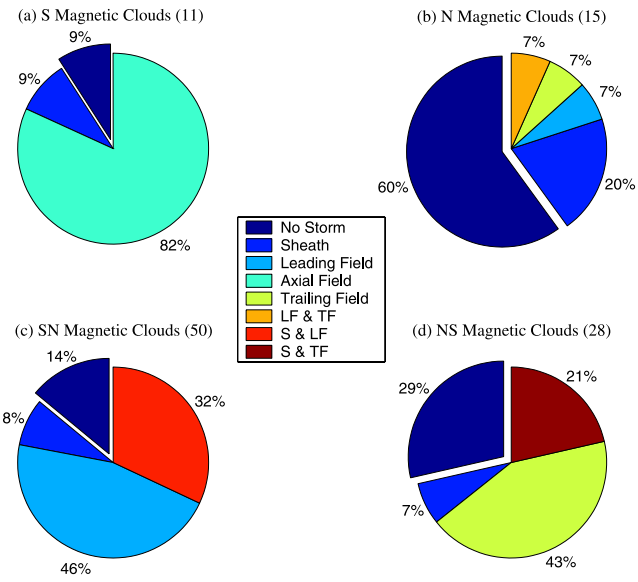

Figure 7. Pie plots showing the occurrence percentages of all levels of geomagnetic activity due to the different fields of "bipolar B_z" and "unipolar B_z" magnetic clouds: (a) S magnetic clouds, (b) N magnetic clouds, (c) SN magnetic clouds, and (d) NS magnetic clouds. The subtotal of each type of magnetic clouds is in parentheses in the respective title.

organized field rotations, but their magnetic cloud signatures do not conform to the strict cloud definition of *Burlaga et al.* [1981]. For example, there are many events that do not undergo a smooth, monotonic IMF rotation over a large angle; either the rotation is over a large angle but is not smooth, i.e., contains considerable fluctuations, or the rotation is smooth, but over a rather small angle (<∼50 degrees in total latitude and longitude). Events in Table 1 whose quality is poor (denoted by "3") are quasi-clouds. Because twenty-four, or 61.5%, of the total thirty-nine quasi-clouds are found to be geoeffective ($Dst^* \leq -30$ nT), as indicated in Table 1, the study of quasi-clouds would be important in space weather predictions.

5.4. Future Work

[40] Much work remains to be done with this data set. For instance, it is of interest to study the statistical differences in B_z strength and longevity observed in the different parts of a magnetic clouds. It is also necessary to investigate the effects of IMF B_y on the solar wind-magnetosphere interactions (including the east and west components in addition to N and S). This could be done by improving our classification of magnetic clouds types from just the B_z component to include the eight B_y-B_z flux-rope field rotation configurations of *Mulligan and Russell* [1998]. With more solar wind observations and geomagnetic indices, it is expected to find cases in which the combinations of the sheath and axial field of magnetic clouds can result in multistep main phase development storms.

[41] **Acknowledgments.** The authors would like to thank the sources of funding for this study: NASA grants NAG5-10297 and NAG-10850 and NSF grant ATM-0090165. T.H.Z. was supported, in part, by NASA contract NAG 5-6921. B.J.L. was supported by the Office of Naval Research and NASA NGT5-50453. The authors would also like to thank the ACE MAG and SWEPAM instrument teams and the ACE Science Center for preparation of the level 2 data available on the ACE Science Center Web site (http://www.srl.caltech.edu/ACE/ASC/), the WDC-C2, Kyoto, for the measured *Dst*, the OMNI Data Center, and Ruth Skoug at LANL for her help with the filling and explanation of some missing ACE data.

[42] Shadia Rifai Habbal thanks Alan J. Lazarus, Slobodan Jurac, and Charles J. Farrugia for their assistance in evaluating this paper.

References

Boteler, D. (1993), Geomagnetically induced currents: Present knowledge and future research, paper presented at IEEE PES Winter Meeting, Inst. of Electr. and Electron. Eng., Columbus, Ohio, 31 Jan. to 5 Feb.

Bothmer, V., and R. Schwenn (1998), The structure and origin of magnetic clouds in the solar wind, *Ann. Geophys.*, *16*, 1.

Burlaga, L. F. (1988), Magnetic clouds and force-free fields with constant alpha, *J. Geophys. Res.*, *93*, 7217–7224.

Burlaga, L. F. (1991), Magnetic clouds, in *Physics of the Inner Heliosphere*, vol. 2, edited by R. Schwenn and E. Marsch, p. 1, Springer-Verlag, New York.

Burlaga, L. F., E. Sittler, F. Mariani, and R. Schwenn (1981), Magnetic loop behind an interplanetary shock: Voyager, Helios, and IMP 8 Observations, *J. Geophys. Res.*, *86*, 6673–6684.

Burlaga, L. F., R. P. Lepping, and J. A. Jones (1990), Global configuration of a magnetic cloud, in *Physics of Magnetic Flux Ropes*, *Geophys. Monogr. Ser.*, vol. 58, edited by C. T. Russell, E. R. Priest, and L. C. Lee, pp. 373–377, AGU, Washington, D. C.

Cane, H. V., and I. G. Richardson (2003), Interplanetary coronal mass ejections in the near-Earth solar wind during 1996–2002, *J. Geophys. Res.*, *108*(A4), 1156, doi:10.1029/2002JA009817.

Cane, H. V., I. G. Richardson, and G. Wibberenz (1997), Helios 1 and 2 observations of particle decrease, ejecta, and magnetic clouds, *J. Geophys. Res.*, *102*, 7075.

Farrugia, C. J., L. F. Burlaga, V. A. Osherovich, and R. P. Lepping (1992), A comparative study of dynamically expanding force-free, constant-alpha magnetic configurations with applications to magnetic clouds, in *Solar Wind Seven*, edited by E. Marsch and R. Schwenn, pp. 611–614, Pergamon, New York.

Farrugia, C. J., L. F. Burlaga, and R. P. Lepping (1997), Magnetic clouds and the quiet-storm effect at Earth, in *Magnetic Storms*, *Geophys. Monogr. Ser.*, vol. 98, edited by B. T. Tsurutani et al., p. 91, AGU, Washington, D. C.

Farrugia, C., et al. (1998), Geoeffectiveness of three Wind magnetic clouds: A comparative study, *J. Geophys. Res.*, *103*(A8), 17,261–17,278.

Goldstein, H. (1983), On the field configuration in magnetic clouds, in *Solar Wind Five*, edited by M. Neugebauer, *NASA Conf. Publ., CP-2280*, pp. 731–733.

Gonzalez, W. D., and B. T. Tsurutani (1987), Criteria of interplanetary parameters causing intense magnetic storms (Dst < −100 nT), *Planet. Space Sci.*, *35*, 1101.

Gonzalez, W. D., J. A. Joselyn, Y. Kamide, H. W. Kroehl, G. Rostoker, B. T. Tsurutani, and V. M. Vasyliunas (1994), What is a geomagnetic storm?, *J. Geophys. Res.*, *99*, 5771–5792.

Gonzalez, W. D., A. L. C. Gonzalez, J. H. A. Sobral, A. D. Lago, and L. Vieira (2001), Solar and interplanetary causes of very intense geomagnetic storms, *J. Atmos. Sol. Terr. Phys.*, *63*, 403–412.

Gosling, J. T. (1990), Coronal mass ejections and magnetic flux ropes in interplanetary space, in *Physics of Magnetic Flux Ropes*, *Geophys. Monogr. Ser.*, vol. 58, edited by C. T. Russell, E. R. Priest, and L. C. Lee, pp. 343–364, AGU, Washington, D. C.

Huttunen, K. E. J., H. E. J. Koskinen, and R. Schwenn (2002), Variability of magnetospheric storms driven by different solar wind perturbations, *J. Geophys. Res.*, *107*(A7), 1121, doi:10.1029/2001JA900171.

Kamide, Y., N. Yokoyama, W. D. Gonzalez, B. T. Tsurutani, I. A. Daglis, A. Brekke, and S. Masuda (1998), Two-step development of geomagnetic storms, *J. Geophys. Res.*, *103*, 6917–6921.

Lepping, R. P., and D. Berdichevsky (2000), Interplanetary magnetic clouds: Sources, properties, modeling, and geomagnetic relationship, in *Recent Research Development in Geophysics*, vol. 3, pp. 77–96, Res. Signpost, Trivandrum-8, India.

Lepping, R. P., J. A. Jones, and L. F. Burlaga (1990), Magnetic field structure of interplanetary magnetic clouds at 1 AU, *J. Geophys. Res.*, *95*, 11,957–11,965.

Lepping, R. P., et al. (2001), The Bastille Day magnetic clouds and upstream shocks: Near-Earth interplanetary observations, *Sol. Phys.*, *204*, 287–305.

Li, Y., and J. Luhmann (2004), Solar cycle control of the magnetic cloud polarity and the geoeffectiveness, *J. Atmos. Sol. Terr. Phys.*, *66*, 323–331.

Lundstedt, H. (1992), Solar caused potential in gas-pipelines in southern Sweden, in *Proceedings of Solar-Terrestrial Workshop in Ottawa May 18–22*, edited by M. A. Shea, pp. 607–610, Natl. Oceanic and Atmos. Assoc., Silver Spring, Md.

Lundstedt, H., P. Wintoft, J.-G. Wu, and H. Gleisner (1995), AI methods and space weather forecasting, paper presented at Artificial Intelligence and Knowledge Based Systems for Space, 5th Workshop, Eur. Space Res. and Technol. Cent., Noordwijk, Netherlands, 10–11 Oct.

Lynch, B. J., T. H. Zurbuchen, L. A. Fisk, and S. K. Antiochos (2003), Internal structure of magnetic clouds: Plasma and composition, *J. Geophys. Res.*, *108*(A6), 1239, doi:10.1029/2002JA009591.

Marubashi, K. (1986), Structure of the interplanetary magnetic clouds and their solar origins, *Adv. Space Res.*, *6*(6), 335–338.

Mulligan, T., and C. T. Russell (1998), Solar cycle evolution of the structure of magnetic clouds in the inner heliosphere, *Geophys. Res. Lett.*, *25*, 2959–2962.

Russell, C. T., R. L. McPherron, and R. K. Burton (1974), On the cause of geomagnetic storms, *J. Geophys. Res.*, *79*, 1105.

Tsurutani, B. T., and W. D. Gonzalez (1997), The interplanetary causes of magnetic storms, in *Magnetic Storms*, *Geophys. Monogr. Ser.*, vol. 98, edited by B. T. Tsurutani et al., pp. 77–89, AGU, Washington, D. C.

Tsurutani, B. T., W. D. Gonzalez, F. Tang, S. I. Akasofu, and E. Smith (1988), Origin of interplanetary southward magnetic fields responsible for major magnetic storms near solar maximum (1978–1979), *J. Geophys. Res.*, *93*, 8519–8531.

Vieira, L. E. A., W. D. Gonzalez, A. L. Clua de Gonzalez, and A. Dal Lago (2001), A study of magnetic storms development in two or more steps and its association with the polarity of magnetic clouds, *J. Atmos. Sol. Terr. Phys.*, *63*, 457–461.

Viljanen, A., and R. Pirjola (1994), Geomagnetically induced currents in the Finnish high-voltage power system, *Surv. Geophys.*, *14*, 383–408.

Wei, F., R. Liu, Q. Fan, and X. Feng (2003), Identification of the magnetic cloud boundary layers, *J. Geophys. Res.*, *108*(A6), 1263, doi:10.1029/2002JA009511.

Wilson, R. M. (1987), Geomagnetic response to magnetic clouds, *Planet. Space Sci.*, *35*, 329.

Wu, C.-C., and R. P. Lepping (2002), Effects of magnetic clouds on the occurrence of geomagnetic storms: The first 4 years of Wind, *J. Geophys. Res.*, *107*(A10), 1314, doi:10.1029/2001JA000161.

Zhang, G., and L. F. Burlaga (1988), Magnetic clouds, geomagnetic disturbances, and cosmic ray decreases, *J. Geophys. Res.*, *93*, 2511–2518.

Zhao, X. P., and J. T. Hoeksema (1998), Central axial field direction in magnetic clouds and its relation to southward interplanetary magnetic field events and dependence on disappearing solar filaments, *J. Geophys. Res.*, *103*(A2), 2077–2083.

Zhao, X. P., and D. F. Webb (2003), Source regions and storm effectiveness of frontside full halo coronal mass ejections, *J. Geophys. Res.*, *108*(A6), 1234, doi:10.1029/2002JA009606.

J. U. Kozyra, M. W. Liemohn, B. J. Lynch, J.-Ch. Zhang, and T. H. Zurbuchen, Space Physics Research Laboratory, University of Michigan, 2455 Hayward Street, #1424, Ann Arbor, MI 48109-2143, USA. (jichunz@umich.edu)